JAERI-M
91-161

SIMPLE DIVERTOR MODEL FOR TRANSPORT ANALYSIS BASED ON EXPERIMENTAL DATA

October 1991

Katsuhiro SHIMIZU, Michiya SHIMADA
and Tomonori TAKIZUKA

日本原子力研究所
Japan Atomic Energy Research Institute

JAERI-Mレポートは，日本原子力研究所が不定期に公刊している研究報告書です。
入手の問合わせは，日本原子力研究所技術情報部情報資料課（〒319-11茨城県那珂郡東海村）あて，お申しこしください。なお，このほかに財団法人原子力弘済会資料センター（〒319-11茨城県那珂郡東海村日本原子力研究所内）で複写による実費頒布をおこなっております。

JAERI-M reports are issued irregularly.
Inquiries about availability of the reports should be addressed to Information Division Department of Technical Information, Japan Atomic Energy Research Institute, Tokai-mura, Naka-gun, Ibaraki-ken 319-11, Japan.

編集兼発行　日本原子力研究所
印　　刷　いばらき印刷㈱

JAERI-M 91-161

Simple Divertor Model for Transport Analysis based on Experimental Data

Katsuhiro SHIMIZU, Michiya SHIMADA and Tomonori TAKIZUKA

Department of Fusion Plasma Research
Naka Fusion Research Establishment
Japan Atomic Energy Research Institute
Naka-machi, Naka-gun, Ibaraki-ken

(Received September 12, 1991)

A simple divertor code has been developed in order to analyze the divertor transport based on the experimental data. The fluid equations are solved numerically in one dimension along the magnetic field lines, neglecting the cross-field diffusion. In contrast to the conventional divertor code, the boundary conditions are given as the fixed plasma parameter at the divertor plate, which are measured by Langmuir probes. The neutral particle transport is treated in two dimensions including the MHD equilibrium and the real wall geometry by a Monte Carlo code. The interaction between the plasma and the neutral particles is solved self-consistently using the iterative procedure. The convergence is very fast compared with the predictive divertor codes because of the fixed plasma parameter at the divertor plate. Short computational time facilitates systematic analysis of divertor transport. Applying this model to the ohmic divertor plasmas in JT-60U initial experiments, the particle confinement time in the main plasma and the heat diffusivity in the scrape-off layer are evaluated.

Keywords: Simple Divertor Model, Transport Analysis, Divertor, JT-60U, Particle Confinement Time, Heat Diffusivity, Neutral Transport

JAERI-M 91-161

実験データに基づく輸送解析のための簡易ダイバータモデル

日本原子力研究所那珂研究所炉心プラズマ研究部
清水　勝宏・嶋田　道也・滝塚　知典

（1991年9月12日受理）

実験データに基づく輸送解析を行うため簡易ダイバータモデルを開発した。磁力線を横切る拡散を無視して，磁力線方向1次元の流体方程式を数値的に解く。従来のダイバータコードと異なり，境界条件として，ダイバータプレートでのプラズマパラメータ（それは，ラングミュアー・プローブで測定される）を固定する。中性粒子の輸送は，実平衡配位と壁の幾何形状を含むモンテカルロコードによって，2次元で扱う。プラズマと中性粒子の相互作用は，繰り返し計算によって，コンシステントに解く。ダイバータプレートでのプラズマパラメータを固定しているため，予測計算を目的としたダイバータコードに比べて，収束は著しく速い。計算時間が，短縮されたため，ダイバータプラズマ輸送を系統的に解析する事が可能となった。このモデルをJT-60Uの初期実験のジュール加熱プラズマに適用して，主プラズマの粒子閉じ込め時間，スクレイプ・オフ層での熱拡散係数を評価した。

那珂研究所：〒311-01　茨城県那珂郡那珂町大字向山801-1

Contents

目　　次

1. Introduction

Understanding of the divertor transport is indispensable for the design works in future tokamaks. A number of divertor codes has been developed to analyze divertor characteristics. In a most elaborate divertor code [1,2,3,4,5], the fluid equations and neutral particle transport is treated in two dimensions. These codes require much labour for development and take much computational time. Because of the complexity of handling these codes, their applications have been restricted to a few cases. In addition, these codes which can predict the divertor characteristics with assumed diffusion coefficients is not convenient for analysis of the observed data.

A simple divertor model has been developed to systematically investigate the divertor transport based on the experimental data. The flow along the magnetic fields dominate the diffusion across the magnetic fields so that the transport behavior of the divertor plasma can be treated in one dimension. The fluid equations along the magnetic field are solved with the boundary conditions of the plasma parameter at the divertor plate (n_d, T_d). In JT-60U experiments, profiles of (n_d, T_d) are measured by a Langmuir probe array. On the other hand, the behavior of neutral particles must be treated in two dimension. The neutral particle transport is simulated in the MHD equilibrium with a real wall geometry by a Monte Carlo code [6]. The interaction between the plasma and neutral particles is solved iteratively, but the plasma parameters reach the steady state after a few iterations. Short computational time facilitates systematic analysis of divertor transport.

This model also provides a method to derive the particle confinement time in the main plasma and the heat diffusivity in the scrape off layer from experimental data. These transport properties are very important to predict the possibility of a cold and dense divertor plasma in future tokamaks. In the conventional predictive divertor transport code, the anomalous cross field diffusion coefficients and particle and heat fluxes flowing into the divertor region must be assumed. The particle confinement time in the main plasma is estimated normally by the integration of H_α-radiation intensity in the whole plasma. When only a small number of channels is available, the H_α radiation profile is determined by using a simple functional form

including several parameters which are adjusted so that the calculated intensity agrees with the experimental data [7]. The H_α radiation near the X-point in the main plasma can not be extracted accurately from the H_α data of the chords viewing the divertor plate. Therefore, the region near the X-point is usually excluded from the estimation of the particle confinement in the main plasma. By using our simple model, the particle confinement time in the main plasma, including the vicinity of the X-point, can be evaluated from the neutral particle flux into the main plasma. As for the cross field diffusion coefficient, $D_\perp$, $\chi_\perp$, in the scrape off layer are usually evaluated from the e-folding length of the measured profiles of density and temperature [8,9]. These measurements by Langmuir probes are not easy in large tokamaks such as JT-60U because of high edge temperature. We propose a method to evaluate the cross field diffusivity $\chi_\perp$ averaged in the scrape off layer from the electron temperature and the cross field heat flux at the divertor entrance ($\overline{DE}$ in Fig.1), which are calculated by our model.

This paper is arranged as follows : In section 2, the simple divertor model is described. Section 3 presents the results of test calculation. The application to JT-60U experiments are presented in section 4. Summary is given in section 5.

2. Simple Divertor Model

We model the divertor region including a part of the scrape-off layer around the main plasma as shown in Fig. 1. The two-dimensional mesh is constructed from the MHD equilibrium and the real wall geometry is used.

2.1 Fluid Equations

The steady state transport equations which describe the divertor plasma are simplified with following assumptions:

* ion temperature is equal to electron temperature,
* the cross field transport effect is negligible,
* the electron heat conduction is the dominant loss in the energy transport.

including several parameters which are adjusted so that the calculated intensity agrees with the experimental data [7]. The H_α radiation near the X-point in the main plasma can not be extracted accurately from the H_α data of the chords viewing the divertor plate. Therefore, the region near the X-point is usually excluded from the estimation of the particle confinement in the main plasma. By using our simple model, the particle confinement time in the main plasma, including the vicinity of the X-point, can be evaluated from the neutral particle flux into the main plasma. As for the cross field diffusion coefficient, $D_\perp$, $\chi_\perp$, in the scrape off layer are usually evaluated from the e-folding length of the measured profiles of density and temperature [8,9]. These measurements by Langmuir probes are not easy in large tokamaks such as JT-60U because of high edge temperature. We propose a method to evaluate the cross field diffusivity $\chi_\perp$ averaged in the scrape off layer from the electron temperature and the cross field heat flux at the divertor entrance ($\overline{DE}$ in Fig.1), which are calculated by our model.

This paper is arranged as follows : In section 2, the simple divertor model is described. Section 3 presents the results of test calculation. The application to JT-60U experiments are presented in section 4. Summary is given in section 5.

2. Simple Divertor Model

We model the divertor region including a part of the scrape-off layer around the main plasma as shown in Fig. 1. The two-dimensional mesh is constructed from the MHD equilibrium and the real wall geometry is used.

2.1 Fluid Equations

The steady state transport equations which describe the divertor plasma are simplified with following assumptions:

* ion temperature is equal to electron temperature,
* the cross field transport effect is negligible,
* the electron heat conduction is the dominant loss in the energy transport.

We employ the orthogonal curvilinear coordinate system (ξ, ζ, ψ) according to reference 5. ξ is the coordinate along the field line, ζ is the coordinate perpendicular to the field line and ψ is the poloidal magnetic flux. The simplified transport equations along the field lines are given as follows,

$$\nabla_{//} (nV_{//}) = S_n \qquad (1)$$

$$\nabla_{//} (nm_i V_{//}^2) + \vec{\nabla}_{//} (2nT) = S_p \qquad (2)$$

$$\nabla_{//} q_{//} = \nabla_{//} (- \kappa_{//} \vec{\nabla}_{//} T) = S_E \qquad (3)$$

where S_n, S_p, and S_E are the particle, momentum, and energy source due to the interaction with the recycling neutrals; n, and T are the density and temperature; $V_{//}$ is the flow velocity parallel to the field lines; m_i is the ion mass. The differential operator are defined as follows,

$$\nabla_{//} = \frac{1}{\sqrt{g}} \frac{\partial}{\partial \xi} (h_\zeta h_\psi) \ ,$$

$$\vec{\nabla}_{//} = \frac{1}{h_\xi} \frac{\partial}{\partial \xi}$$

The metric coefficients of h_ξ , h_ζ , h_ψ and $\sqrt{g} = h_\xi h_\zeta h_\psi$ are calculated from the MHD equilibrium. $q_{//}$ is the electron heat conduction parallel to the field lines and $\kappa_{//}$ is the classical electron heat diffusivity along the field lines.

$$\kappa_{//} = \kappa_0 T^{5/2}$$

$$\kappa_0 = 3.07 \times 10^4 / \ln \Lambda \qquad (4)$$

where $\kappa_{//}$ is in W $(eV)^{-1}$ m^{-1} unit and $\ln \Lambda$ is the Coulomb logarithm.

By integration of eq. (3) along a field line, $q_{//}$ is calculated by

$$q_{//}(\xi) = \frac{1}{A(\xi)} \left\{ A(\xi_d) \cdot q_{//}(\xi_d) - \int_{\xi}^{\xi_d} S_E \, dV \right\} \qquad (5)$$

where $A(\xi)$ is the area of the cross section of a flux tube; dV is the volume element of the flux tube between ξ and $\xi + d\xi$, and ξ_d corresponds to the divertor plate. The heat flux at the plate, $q_{//}(\xi_d)$ is given by the sheath condition,

$$q_{//}(\xi_d) = \gamma \, n_d \, T_d \, V_{//d} \qquad (6)$$

where n_d, and T_d are the density and temperature at the plate, γ is the heat transmission coefficient. n_d, and T_d which are measured by the Langmuir probes are given as the input data. Integration of eq. (5) gives the electron temperature profile along the field lines,

$$T^{7/2}(\xi) = T_d^{7/2} + \frac{7}{2 \kappa_0} \int_{\xi}^{\xi_d} q_{//}(\xi) \, dL \qquad (7)$$

where L is the distance along the field line.

The particle flux parallel to the field lines, $f_{//} = nV_{//}$ is calculated by the integration of equation (1).

$$f_{//}(\xi) = \frac{1}{A(\xi)} \left\{ A(\xi_d) \cdot f_{//}(\xi_d) - \int_{\xi}^{\xi_d} S_n \, dV \right\} \qquad (8)$$

where $f_{//}(\xi_d)$ is calculated from the ion saturation current of Langmuir probes. Integration of eq. (2) results in

$$A(\xi)\, n(\xi)\, T(\xi)\, M^2(\xi) = A(\xi_d)\, n_d\, T_d - \int_{\xi}^{\xi_d} \frac{\partial}{\partial L}(n\,T)\, dV - \int_{\xi}^{\xi_d} \frac{1}{2} S_p\, dV \tag{9}$$

where $M(\xi) = V_{//} / C_S$ is the Mach number and $C_S = \sqrt{2T / m_i}$ is the sound velocity. In this derivation, the Bohm condition ($M(\xi_d) = 1$) is used. Changing the second term in the right-hand side, the equation (9) becomes a more familiar form:

$$A(\xi)\, n(\xi)\, T(\xi) \left\{1 + M^2(\xi)\right\} = A(\xi_d)\, 2\, n_d\, T_d - \int_{\xi}^{\xi_d} \frac{\partial A}{\partial L} n\, T\, dL - \int_{\xi}^{\xi_d} \frac{1}{2} S_p\, dV \tag{9b}$$

However, the equation (9) is more convenient for the numerical integration. Substituting $n = f_{//} \sqrt{m_i / 2T} / M$ into eq (9), the quadratic equation of $M(\xi)$ is obtained. Physical parameters are defined at difference mesh (ξ_i, i = 1, 2, ..., I_d)

$$A_i \cdot M_i^2 - \left\{ \frac{f_{//i+1}}{f_{//i}} \left(\frac{T_{i+1}}{T_i}\right)^{1/2} \cdot \frac{1}{M_{i+1}} \left(A_{i+1/2} + A_{i+1}\, M_{i+1}^2 \right) - \frac{1}{2} \frac{C_i}{f_{//i}} \frac{1}{T_i} S_{p\, i+1/2}\, \Delta V_{i+1/2} \right\} \cdot M_i + A_{i+1/2} = 0 \tag{10}$$

where M_i is Mach number at ξ_i and $A_{i+1/2} \equiv (V(\xi_{i+1}) - V(\xi_i)) / (L(\xi_{i+1}) - L(\xi_i))$ is the average area of the cross section of the flux tube between ξ_i and ξ_{i+1} . $M(\xi)$ and $V_{//}(\xi)$ are determined from the divertor plate to the upstream by solving equation (10) under the subsonic condition of $v_{//} < C_s$. The density is finally obtained from

$$n = f_{//} / v_{//} \tag{11}$$

The density and temperature are calculated in each flux tube for given source terms (S_n, S_p, S_E).

2.2 Neutral Transport

We use a 2-D Monte Carlo code in order to obtain the neutral density profile and the source terms. Neutral particles are generated at the divertor plate by the recycling of the plasma ions. They are traced considering the ionization and charge-exchange processes and the wall reflection. The algorithm to estimate the neutral density uses the path length estimator method [10]. The reflection model for ions at the divertor plate and neutral particles at the wall is similar to that in reference [6]. The neutral particles which escape into the main plasma are reflected on the separatrix surface ($\overline{CD}$ in Fig. 1) with a reflection coefficient. This value is chosen so as to simulate reentering particles into the divertor region by the charge-exchange in the main plasma. We use a mirror reflection model on the separatrix surface from the divertor plate to the X-point ($\overline{BC}$), in order to simulate the neutral particles generated at the inside divertor plate. The particles escaping through the scrape off layer ($\overline{DE}$) or the void ($\overline{EG}$) are also reflected with the reflection coefficient of 0.1. This value has little influence on our calculation results.

The source term S_n is calculated from

$$S_n = n_e\, n_0\, \langle \sigma v \rangle_i \qquad (12)$$

where $n_e = n$, n_0 is the neutral density and $\langle \sigma v \rangle_i$ is the ionization reaction rates. Monte Carlo scoring is not used for the estimation of S_n because of a large variance. The energy loss term S_E due to electron ionization is expressed by

$$S_E = - E_{ion}\, S_n \qquad (13)$$

where E_{ion} is the ionization potential. We take the radiation loss of impurities effectively by the enhancement of E_{ion} by a factor of 3 ~ 4.

2.3 Interaction between Plasma and Neutral Particles

The interaction between the plasma and neutral particles are iteratively solved. From the viewpoint of the computational time, our code is also superior to the full 2D divertor codes. The convergence towards the steady state solution is very fast, because the plasma parameters at the plate (n_{ed}, T_{ed}) are fixed as the boundary condition. On the other hand, in the predictive

divertor code, T_{ed} is determined from the sheath condition [11] and it changes every iteration. It should be noted that the behavior of the plasma flow and neutral particles is sensitive to the edge parameters. The change of T_{ed} has a strong effect on the neutral transport through the reflection energy of recycled neutrals at the divertor plate. These effects demand many iterations before reaching the steady state in the predictive divertor code.

3. Test calculations

We have checked whether the fluid equations can be solved correctly from the divertor plate to the upstream as described in the previous section. The divertor plasma parameters for this test are obtained by solving the fluid equations with the boundary conditions of particle and heat fluxes fixed at the entrance. We describe this procedure as follows.

We introduce the difference mesh along the magnetic field lines ξ_i i = 1, 2, ..., I. The entrance and the divertor plate correspond to i = 1 and i = I, respectively. The plasma parameter (n, T, $V_{//}$) are defined at the integral mesh ξ_i . On the other hand, auxiliary parameter $q_{//}$ and the source terms (S_n, S_p, S_E) are defined at the half integral mesh $\xi_{i+1/2}$ i = 1, 2, ..., I-1. The recurrence formula for particle and heat flux are obtained by integrating the equation (1) and (3) in the flux tube between ξ_i and ξ_{i+1} .

step 1 : particle flux

$f_{//1}$: given

$$A_{i+1}\, f_{i+1} = A_i\, f_i + S_{n\, i+1/2}\, \Delta V_{i+1/2} \qquad i = 1, 2, ..., I-1$$

where $\Delta V_{i+1/2}$ is the volume element.

step 2 heat flux

$q_{//1}$: given

$$A_{3/2}\, q_{//3/2} = A_1\, q_{//1} + \frac{1}{2} S_{E\, 3/2}\, \Delta V_{3/2}$$

$$A_{i+1/2}\, q_{//i+1/2} = A_{i-1/2}\, q_{//i-1/2} + \frac{1}{2} \left(S_{E\, i-1/2}\, \Delta V_{i-1/2} + S_{E\, i+1/2}\, \Delta V_{i+1/2} \right)$$

$$i = 2, 3, ..., I-1$$

divertor code, T_{ed} is determined from the sheath condition [11] and it changes every iteration. It should be noted that the behavior of the plasma flow and neutral particles is sensitive to the edge parameters. The change of T_{ed} has a strong effect on the neutral transport through the reflection energy of recycled neutrals at the divertor plate. These effects demand many iterations before reaching the steady state in the predictive divertor code.

3. Test calculations

We have checked whether the fluid equations can be solved correctly from the divertor plate to the upstream as described in the previous section. The divertor plasma parameters for this test are obtained by solving the fluid equations with the boundary conditions of particle and heat fluxes fixed at the entrance. We describe this procedure as follows.

We introduce the difference mesh along the magnetic field lines ξ_i i = 1, 2, ..., I. The entrance and the divertor plate correspond to i = 1 and i = I, respectively. The plasma parameter (n, T, $V_{//}$) are defined at the integral mesh ξ_i . On the other hand, auxiliary parameter $q_{//}$ and the source terms (S_n, S_p, S_E) are defined at the half integral mesh $\xi_{i+1/2}$ i = 1, 2, ..., I-1. The recurrence formula for particle and heat flux are obtained by integrating the equation (1) and (3) in the flux tube between ξ_i and ξ_{i+1} .

step 1 : particle flux

$f_{//1}$: given

$$A_{i+1}\, f_{i+1} = A_i\, f_i + S_{n\, i+1/2}\, \Delta V_{i+1/2} \qquad i = 1, 2, ..., I-1$$

where $\Delta V_{i+1/2}$ is the volume element.

step 2 heat flux

$q_{//1}$: given

$$A_{3/2}\, q_{//3/2} = A_1\, q_{//1} + \frac{1}{2} S_{E\, 3/2}\, \Delta V_{3/2}$$

$$A_{i+1/2}\, q_{//i+1/2} = A_{i-1/2}\, q_{//i-1/2} + \frac{1}{2} \left(S_{E\, i-1/2}\, \Delta V_{i-1/2} + S_{E\, i+1/2}\, \Delta V_{i+1/2} \right)$$

$$i = 2, 3, ..., I-1$$

step 3 temperature

$$T_I = q_{//I} / \gamma f_{//I}$$

$$T_i^{7/2} = T_{i+1}^{7/2} + \frac{7}{2\kappa_0} q_{// i+1/2} \Delta L_{1+1/2} \qquad i = I-1, I-2, ..., 1$$

The recurrence formula for flow velocity is obtained by integrating the equation (2) in the flux tube between ξ_i and ξ_{i+1} .

$$n_i T_i (A_{i+1/2} + A_i M_i^2) = n_{i+1} T_{i+1} (A_{i+1/2} + A_{i+1} M_{i+1}^2) - \frac{1}{2} S_{p\ 1+1/2} \Delta V_{i+1/2}$$

where $A_{i+1/2} \equiv \Delta V_{i+1/2} / \Delta L_{i+1/2}$. Substituting $n = f_{//} \sqrt{m_i / 2T} / M$ into above equation, the relation between M_i and M_{i+1} is obtained.

step 4 flow velocity

$$M_I = 1.0$$

$$A_i \cdot M_i^2 - \left\{ \frac{f_{//i+1}}{f_{//i}} \left(\frac{T_{i+1}}{T_i} \right)^{1/2} \cdot \frac{1}{M_{i+1}} \left(A_{i+1/2} + A_{i+1} M_{i+1}^2 \right) - \frac{1}{2} \frac{C_i}{f_{//i}} \frac{1}{T_i} S_{p\ i+1/2} \Delta V_{i+1/2} \right\} \cdot M_i + A_{i+1/2} = 0$$

$$i = I-1, I-2, ..., 1$$

step 5 density

$$n_i = f_{//\,i} \sqrt{m / 2T_i} / M_i$$

$$i = 1,2 , ..., I$$

The above is the procedure to solve the fluid equations for the case where the particle and heat fluxes at the throat are specified as the boundary conditions.

The calculation is done for the rectangular divertor which is used in reference [12], as shown in Fig. 2. Figure 3 shows the calculated plasma parameters as a function of poloidal length. The particle and heat fluxes are 3.5×10^{20} s^{-1} and 27 MW , respectively. The density increases from 0.6×10^{20} m^{-3} at the throat up to 2×10^{20} m^{-3} at the front of the divertor plate. The temperature decreases from 62 eV at the throat to 15 eV at the divertor plate. The flux amplification factor reaches 25. These results demonstrate the possibility of a cold and dense divertor plasma even in discharges with high heating power of ~ 30 MW. Our results are

consistent with those of reference [12] which are plotted by broken lines in Fig. 3. The comparison were performed for the various particle fluxes, as shown in Fig. 4. Our results are shown by open and closed symbols. The agreement is fairly good. The small discrepancy is due to the difference of the radiation model. In our model, the radiation profile is calculated by the enhancement of the ionization potential E_{ion} so that the total radiation power may agree with the given value. In the reference [12], the radiation profile were calculated from the cooling rate [13] with an assumed impurity concentration of 1.25 %.

Figure 5 shows the plasma parameters which are calculated using the boundary condition at the divertor plate of $n_d = 1.3 \times 10^{19}$ m^{-3} and $T_d = 15$ eV. They are plotted by open symbols. The solid lines are the plasma parameters which are solved with the boundary condition of the particle and heat fluxes at the throat. The agreement is so good that the difference can not be recognized. This solution which includes the interaction between the neutral particles and the plasma is obtained after two or three iterations. This result confirms the validity of our calculation method.

4. Application to JT-60U Experiments

4.1 Experimental Data

We investigate the divertor transport in the ohmic experiments ($I_p = 2$ MA, $B_T = 3.5$ T, $\bar{n}_e = 0.8 \sim 3.0 \times 10^{19}$ m^{-3}) using our simple divertor model.

The 15 channel Langmuir probes are installed on the divertor plates. The measured profiles of ion saturation current I_s, and temperature T_d, are fitted by using the function of exp ($-x / \lambda$) with exponential decay length, λ_I and λ_T , respectively. The smoothed density is obtained by

$$n_d = \frac{I_s}{e\,S}\sqrt{\frac{m_i}{2\,T_d}} \qquad (14)$$

where S is the effective area of a probe. Typical radial profiles of n_d and T_d are shown for a high temperature case (shot no # 12953) and a low temperature case (shot no # 12956) in Fig. 6 (a) and Fig. 7(a), respectively. These data are displayed by closed symbols at the position corresponding to the radial distance from the separatrix surface at the entrance ($\overline{DE}$).

4.2 Calculated Plasma Parameter

The numerical simulations has been carried out for the outside divertor plasma, which is divided into 8 flux tubes, as shown in Fig. 1. In the present paper, we assume that the momentum source term is negligible and $v_{//} << C_s$ for simplicity. In this case, the density is calculated directly from the condition of constant pressure.

$$n = 2\,n_d\,T_d / T \qquad (15)$$

The closed symbols denote the measured values and the broken line denotes the fitted profile which is used as the input data of our simple divertor model. Figure 6(b) shows the profiles of the density and temperature in the flux tube close to the separatrix surface for the high temperature case. These profiles are those projected on the poloidal cross section. (z is the poloidal coordinate.) The temperature gradient along the field line is extremely small due to the high thermal conductivity. The low density and high temperature at the plate imply a long mean

free path of recycled neutrals; the density buildup is not observed. For the low temperature case, the distribution of plasma parameters along the field line close to the separatrix surface is shown in Fig. 7(b). The temperature gradient and the high density near the divertor plate are obtained due to the low temperature. The temperature gradient appears when the high recycling is realized or the temperature is low due to the low heat flux. We consider the threshold temperature in the latter case. Neglecting the change of $A(\xi)$ and the ionization loss term, which is negligible because of low recycling, the electron temperature is expressed by

$$T^{7/2}(\xi) = T_d^{7/2} + \frac{7}{2\kappa_0} q_{//}(\xi_d)\, L_d \qquad (16)$$

where L_d is the distance from the X-point to the divertor plate along the field line. Then the temperature gradient appears when the first term in the right hand side is small compared with the second term.

$$T_d < (2.4 \times 10^{-17}\, n_d\, L_d)^{1/2} \qquad (17)$$

where T_d is in eV unit. Substituting $L_d \cong 5$ m and the density at the plate, the threshold temperature are about 10 eV and 30 eV for Fig. 6(b) and Fig. 7(b), respectively. The difference of the spatial dependence of $T(\xi)$ can be well explained by the threshold given by eq. (17). The variation of n (z) and T (z) in the upstream ($z \leq 0.5$ m) is small. This indicates that the calculation region is so long that the calculation results are insensitive to the length of the system. The total particle flux, Γ (0) and heat flux, Q (0) at z=0 are 2.5×10^{22} s^{-1} and 0.49 MW, respectively. About 40 ~ 50 % of joule input power (~ 1 MW) is lost by the radiation loss in the main plasma. Then Q (0) is consistent with the experimental data.

4.3 Comparison with H_α Measurement

In order to check the validity of our model, Calculated H_α-intensities are compared with the measured intensities. The H_α monitor viewing the divertor plate consists of 38 channels , as shown in Fig. 8. The H_α radiation intensity is calculated by

$$I(H_\alpha) = \frac{1}{4\pi}\int_{path} S_n \,/\, \varepsilon(n_e, T_e)\, dl \qquad (18)$$

where $\varepsilon(n_e, T_e)$ is the ionization events per H_α emission, which is calculated from the collisional-radiative model [14]. The closed symbols are measured intensities and the solid line is the calculated profile. They are in good agreement except for the chord passing near the X-point ($R \approx 3.0$ m). This discrepancy is due to the H_α radiation in the main plasma. The ions recycled at the plate are mostly reflected in the direction of the normal to the plate and probability of ionization in the divertor plasma is not so large (~ 70 % even in the low temperature case). The attenuation of neutral density at the X-point is about 1 order even in the low temperature case. It follows that H_α emission near the X-point in the main plasma is not negligible . The H_α calculation including the main plasma, especially near the X-point, is left for future work. The agreement in general implies that our simple model is reasonable.

4.4 Estimation of Particle Confinement

The data of H_α monitor shows that the neutral particle recycling is localized near the X-point (see Fig. 8). Then other sources of neutral particles, i.e. the gas fuelling, the recycling of the wall and the recombination, can be neglected. The results of the particle confinement time evaluated are summarized in Table 1. The total particle flux to divertor plates, including the inside plate, $\Gamma_e(L_d)$ increases with density in the main plasma. The flux amplification factor, $R = \Gamma_e(L_d) / \Gamma_e(0)$, is below 2 because of the low density. The neutral particle flux back flow into the main plasma , Γ_0 (M) shows a tendency to saturate. The particle confinement time including the divertor region, τ_p (D) are nearly constant (45 ~ 50 msec). On the other hand, the particle confinement time in the main plasma, τ_p (M), estimated from Γ_0 (M) increases from

71 msec to 108 msec with increase of main plasma density. This density dependence of τ_p (M) is generally observed in the low density regime [15.

4.5 Estimation of Cross Field Heat Diffusivity

Let us consider the energy balance in the scrape off layer close to separatrix surface. This flux tube starts from the symmetric surface and ends at the entrance ($\overline{DE}$). Temperature and density can be considered to be constant in this region (see Fig. 6, 7). The total heat flux $Q_\perp(0)$ which flows into this region across the separatrix surface is equal to the total heat flux into the divertor region, assuming that the energy loss term can be neglected in the scrape-off layer around the main plasma.

$$Q_\perp(0) = \sum_{i=1}^{8} q_{//}(i) \cdot A(i) \qquad (19)$$

where A(i) is the cross section of the flux tube, $q_{//}(i)$ is the heat flux parallel to the field line, index of i is the number of the flux tube. A part of $Q_\perp(0)$ diffuses to the next flux tube due to the cross field diffusion. This heat flux is $Q_\perp(1) = Q_\perp(0) - q_{//}(1)\, A(1)$. So that $\chi_\perp$ is evaluated by

$$\chi_\perp(1) = \frac{Q_\perp(0) - q_{//}(1)\, A_{//}(1)}{B\, n(1)\, (\, T(1) - T(2)\,) / \Delta x} \qquad (20)$$

where B is the total surface of the plasma and Δx is the averaged distance between the flux tubes. The heat diffusivity evaluated is almost constant and is ~ 3 m^2/s for the density range investigated, as shown in Table 1. The ratio of the divergence of the cross field heat flux to that of the parallel heat flux, $\nabla_\perp \cdot q_\perp / \nabla_{//} \cdot q_{//}$ in the divertor plasma is approximately expressed by

$$\nabla_\perp \cdot q_\perp / \nabla_{//} \cdot q_{//} \sim \frac{n\chi}{\Delta x}\frac{\Delta T}{\Delta x} \Big/ \frac{\Delta q_{//}}{L_d} \qquad (21)$$

where $\Delta q_{//}$ is the difference between the parallel heat flux at the plate and that at the throat ($\overline{CF}$ in Fig. 1). Using the calculated profiles of T and $q_{//}$ and the evaluated $\chi_{\perp}$, we estimate this ratio to be below 0.1. This argument justifies the assumption that the cross-field heat flux is negligible.

5. Summary

We have developed a simple divertor code which analyzes the divertor transport based on the experimental data. The one-dimensional fluid equations along the field line are solved numerically with the boundary condition of the plasma parameters given at the divertor plate by the Langmuir probe data. The neutral particle transport is simulated in a two dimensional geometry by a Monte Carlo code. The fast convergence towards the steady state solution facilitates systematic analysis of divertor transport.

Applying this model to the ohmic divertor plasmas in JT-60U initial experiments, the particle confinement time in the main plasma and the heat diffusivity in the scrape-off layer are evaluated.

Acknowledgments

The authors would like to thank Drs. Y. Shimomura and M. Azumi for their fruitful discussions and encouragements. They also wish to acknowledge valuable discussions with Dr. K. Itoh. They are indebted to Drs. K. Itami and N. Asakura for Langmuir probe data and to Dr. H. Kubo for H_{α}-radiation data.

where $\Delta q_{//}$ is the difference between the parallel heat flux at the plate and that at the throat ($\overline{CF}$ in Fig. 1). Using the calculated profiles of T and $q_{//}$ and the evaluated $\chi_{\perp}$, we estimate this ratio to be below 0.1. This argument justifies the assumption that the cross-field heat flux is negligible.

5. Summary

We have developed a simple divertor code which analyzes the divertor transport based on the experimental data. The one-dimensional fluid equations along the field line are solved numerically with the boundary condition of the plasma parameters given at the divertor plate by the Langmuir probe data. The neutral particle transport is simulated in a two dimensional geometry by a Monte Carlo code. The fast convergence towards the steady state solution facilitates systematic analysis of divertor transport.

Applying this model to the ohmic divertor plasmas in JT-60U initial experiments, the particle confinement time in the main plasma and the heat diffusivity in the scrape-off layer are evaluated.

Acknowledgments

The authors would like to thank Drs. Y. Shimomura and M. Azumi for their fruitful discussions and encouragements. They also wish to acknowledge valuable discussions with Dr. K. Itoh. They are indebted to Drs. K. Itami and N. Asakura for Langmuir probe data and to Dr. H. Kubo for H_{α}-radiation data.

where $\Delta q_{//}$ is the difference between the parallel heat flux at the plate and that at the throat ($\overline{CF}$ in Fig. 1). Using the calculated profiles of T and $q_{//}$ and the evaluated $\chi_{\perp}$, we estimate this ratio to be below 0.1. This argument justifies the assumption that the cross-field heat flux is negligible.

5. Summary

We have developed a simple divertor code which analyzes the divertor transport based on the experimental data. The one-dimensional fluid equations along the field line are solved numerically with the boundary condition of the plasma parameters given at the divertor plate by the Langmuir probe data. The neutral particle transport is simulated in a two dimensional geometry by a Monte Carlo code. The fast convergence towards the steady state solution facilitates systematic analysis of divertor transport.

Applying this model to the ohmic divertor plasmas in JT-60U initial experiments, the particle confinement time in the main plasma and the heat diffusivity in the scrape-off layer are evaluated.

Acknowledgments

The authors would like to thank Drs. Y. Shimomura and M. Azumi for their fruitful discussions and encouragements. They also wish to acknowledge valuable discussions with Dr. K. Itoh. They are indebted to Drs. K. Itami and N. Asakura for Langmuir probe data and to Dr. H. Kubo for H_{α}-radiation data.

Reference

[1] PETRAVIC, M., POST, D., HEIFETZ D., SCHMIDT, J., Phys. Rev. Lett. 48, 326(1982).

[2] BRAAMS, B.J., in Controlled Fusion and Plasma Physics (Proc. 11 th Eur. Conf. Aschen, 1983), Vol. 7D, Part II, European Physical Society (1983) 431.

[3] SAITO, S., SUGIHARA, M., FUJISAWA, N., J. Nucl. Mater. **121** (1984) 199.

[4] UEDA, N., et al., Nucl. Fusion **28** (1988) 1183.

[5] PETRAVIC, M., KUO-PETRAVIC, G., Nucl. Fusion 30 (1990) 1148.

[6] SEKI, Y., SHIMOMURA, Y., MAKI, K., AZUMI, M., TAKIZUKA, T., Nucl. Fusion **20** (1980) 1213.

[7] YAMADA, K.., TSUJI, S., SHIMIZU, K., NISHITANI, T., NAGASHIMA, K., the JT-60 TEAM, Nucl. Fusion **27** (1987) 1203.

[8] UEHARA, K., GOMAY, Y., YAMAMOTO, T., SUZUKI, N., MAENO, M., et al., Plasma Phys. **21** (1979) 89.

[9] STANGEBY, P.C., TAGLE, J.A., ERENTS, S.K., LOWRY, C., Plasma Phys. Controlled Fusion **30** (1988) 1787.

[10] SHIMIZU, K., AZUMI, M., Two Dimensional Neutral Transport Analysis in Tokamak Plasma, JAERI-M 87-028 (1987) [in Japanese].

[11] HOBBS, G.D., WESSON, J.A., Plasma Physics **9** (1967) 85.

[12] YOSHIDA, H., SHIMIZU, K., AZUMI, M., Numerical Studies on JT-60 Divertor Plasma Characteristics, JAERI-M 86-008 (1986) [in Japanese].

[13] SHIMADA, M., JAERI-M 82-195 (1982).

[14] JOHNSON, L.C., HINNOV, E., J. Quant. Spectros. Radiat. Transfer **13** (1973) 333.

[15] WOOTTON, A.J., et al., Plasma Phys. Controlled Fusion **30** (1988) 1479.

Table 1 Estimation of Particle Confinement Time and Heat Diffusivity

shot no	12953	12956	12959
$\overline{n_e}$	0.8×10^{19} m^{-3}	1.8×10^{19} m^{-3}	2.7×10^{19} m^{-3}
$n_e(L_d)$	1.0×10^{18} m^{-3}	7.1×10^{18} m^{-3}	8.9×10^{18} m^{-3}
$T_e(L_d)$	~84 eV	~9 eV	~9 eV
$n_0(L_d)$	2.0×10^{17} m^{-3}	6.0×10^{17} m^{-3}	7.5×10^{17} m^{-3}
$\Gamma_e(L_d)$	1.6×10^{22} s^{-1}	4.1×10^{22} s^{-1}	5.0×10^{22} s^{-1}
$\Gamma_e(0)$	1.2×10^{22} s^{-1}	2.5×10^{22} s^{-1}	2.8×10^{22} s^{-1}
$R = \Gamma_e(L_d) / \Gamma_e(0)$	1.4	1.7	1.8
Γ_0 (M)	1.0×10^{22} s^{-1}	2.0×10^{22} s^{-1}	2.3×10^{22} s^{-1}
τ_p(D)	44 msec	40 msec	49 msec
τ_p(M)	71 msec	79 msec	108 msec
$\chi_\perp(x=0)$	3.4 m^2/s	3.3 m^2/s	3.0 m^2/s

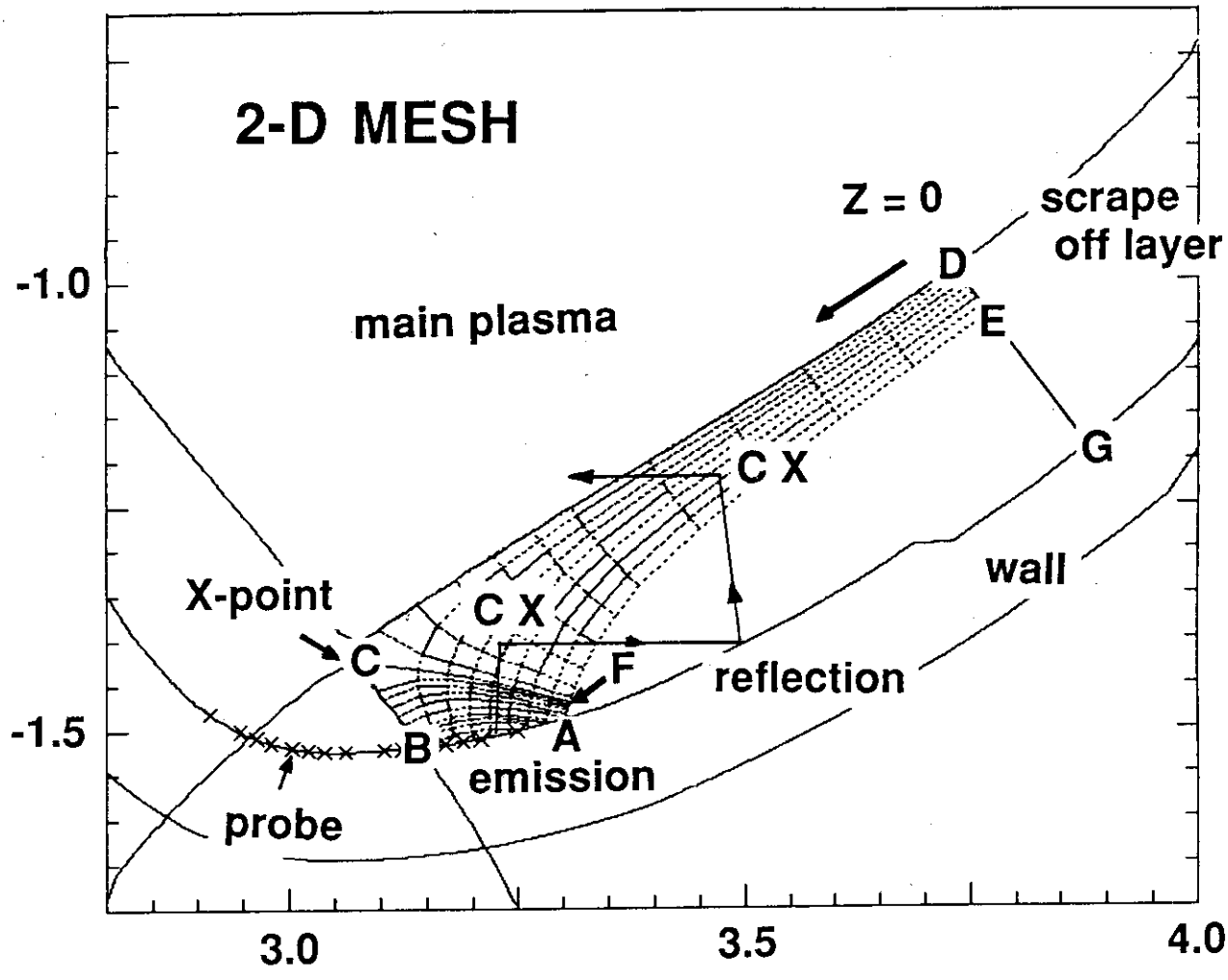

Fig.1 Two dimensional computational mesh. The outside divertor plasma together with the scrape off layer is modeled and is divided into the 8 flux tubes.

Calculation Parameters

L1 = 100 cm, L2 = 30 cm, L3 = 30 cm

δ_{void} = 3 cm, f_{pump}= 0.2, θ = 0.127

$\Gamma_{th} = 3.5 \times 10^{22}$ s^{-1}, Q_{th} = 27 MW

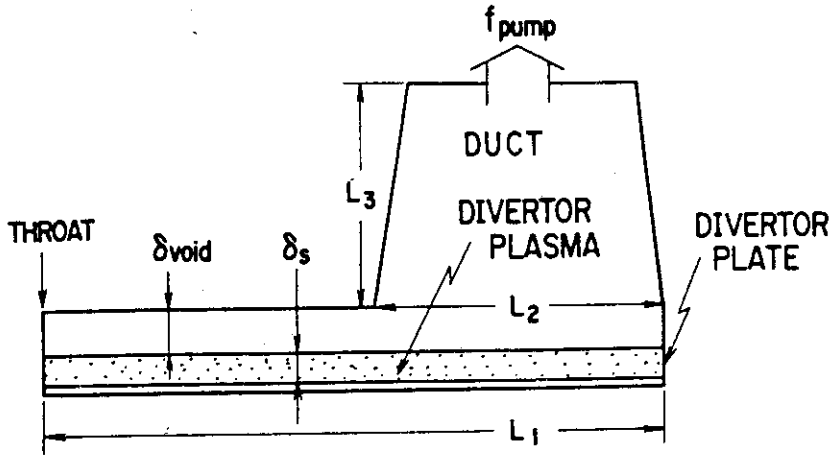

Fig. 2 Model of divertor plasma and calculation parameters.

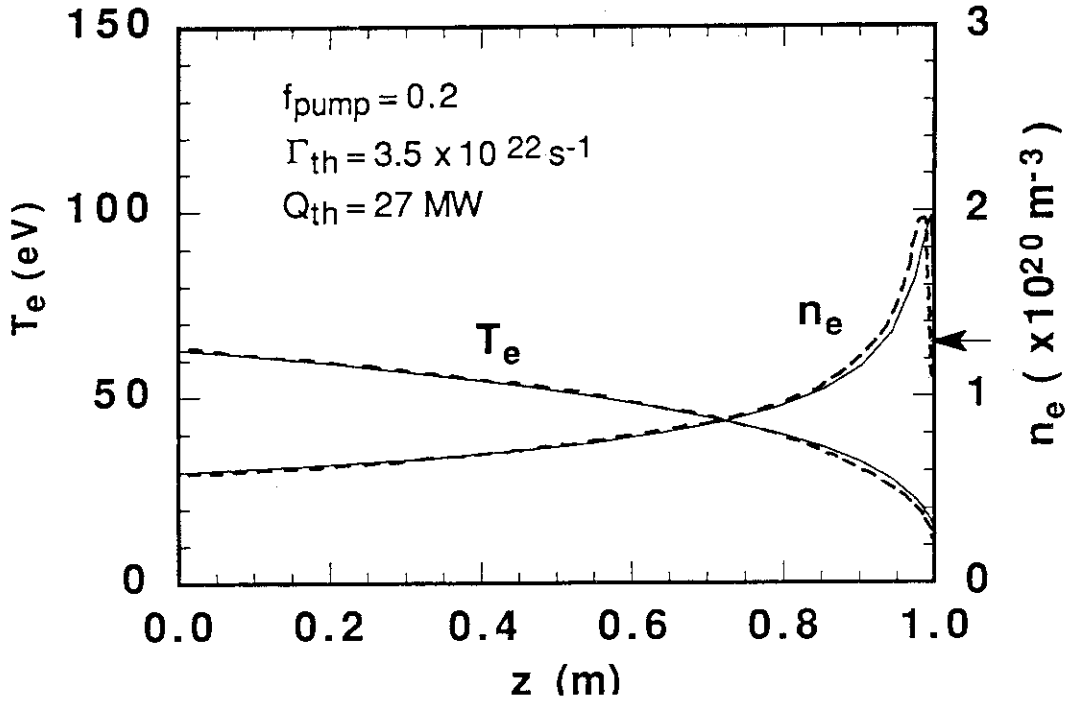

Fig. 3 Calculated profiles of temperature and density.

The total particle and heat fluxes are 3.5×10^{20} s^{-1} and 27 MW , respectively. The results in reference [11] are shown by broken lines.

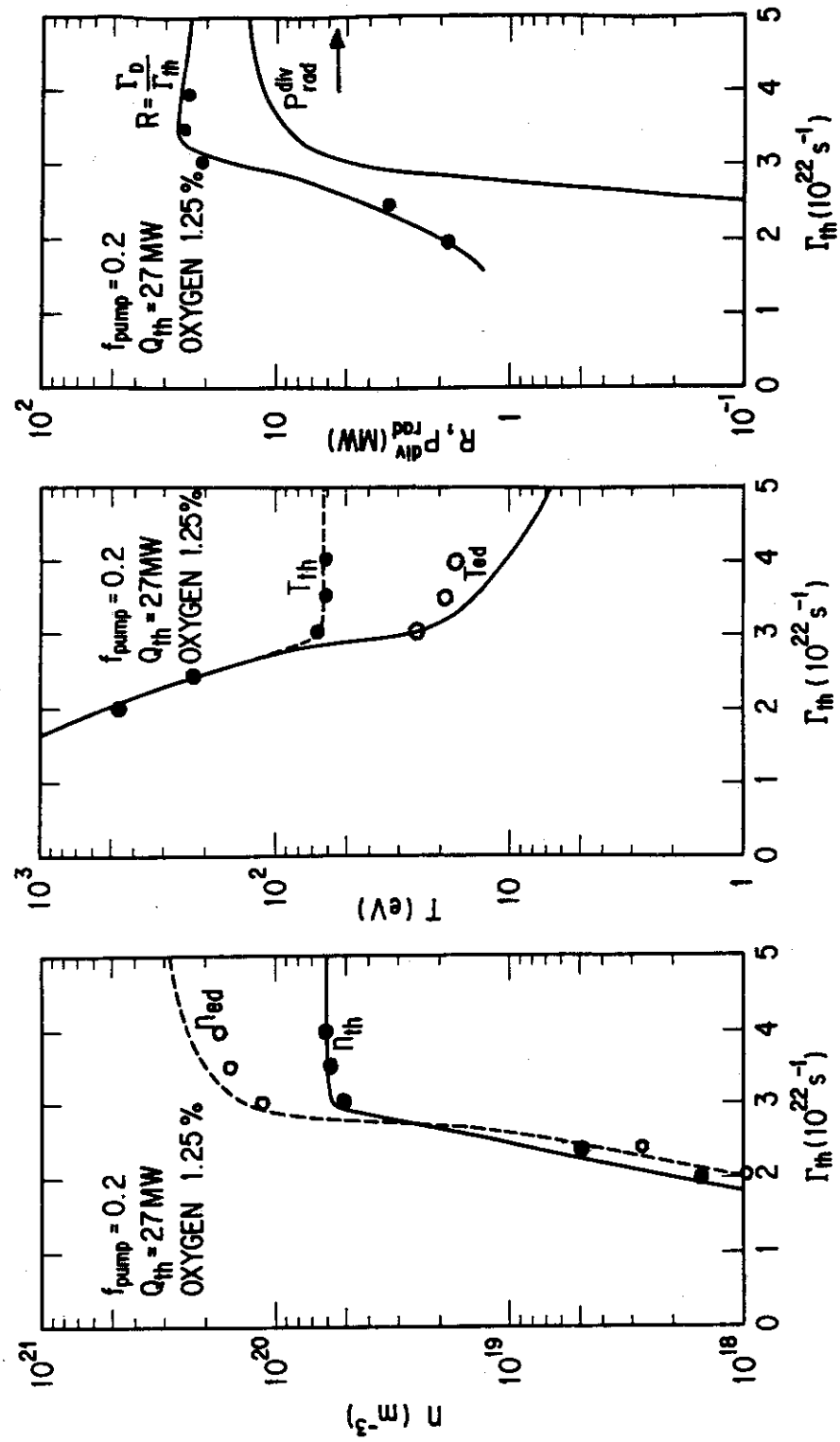

Fig. 4 Divertor characteristics for the fixed heat flux Q_{th} = 27 MW.

Open and closed symbols denote our results and lines denote the results in reference [11].

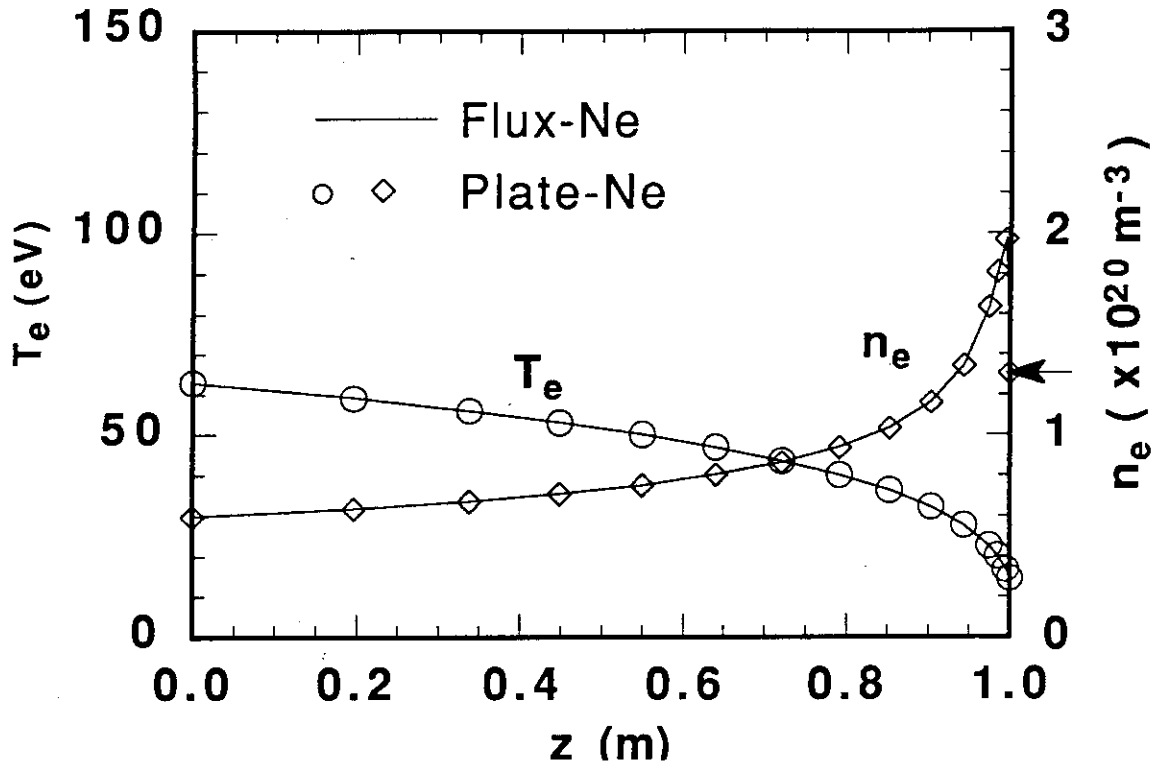

Fig. 5 Comparison of plasma parameters calculated by two different methods which associate with the boundary conditions. Open symbols corresponds to solution with the boundary condition at the divertor plate and solid lines corresponds to solutions with the boundary condition at the throat.

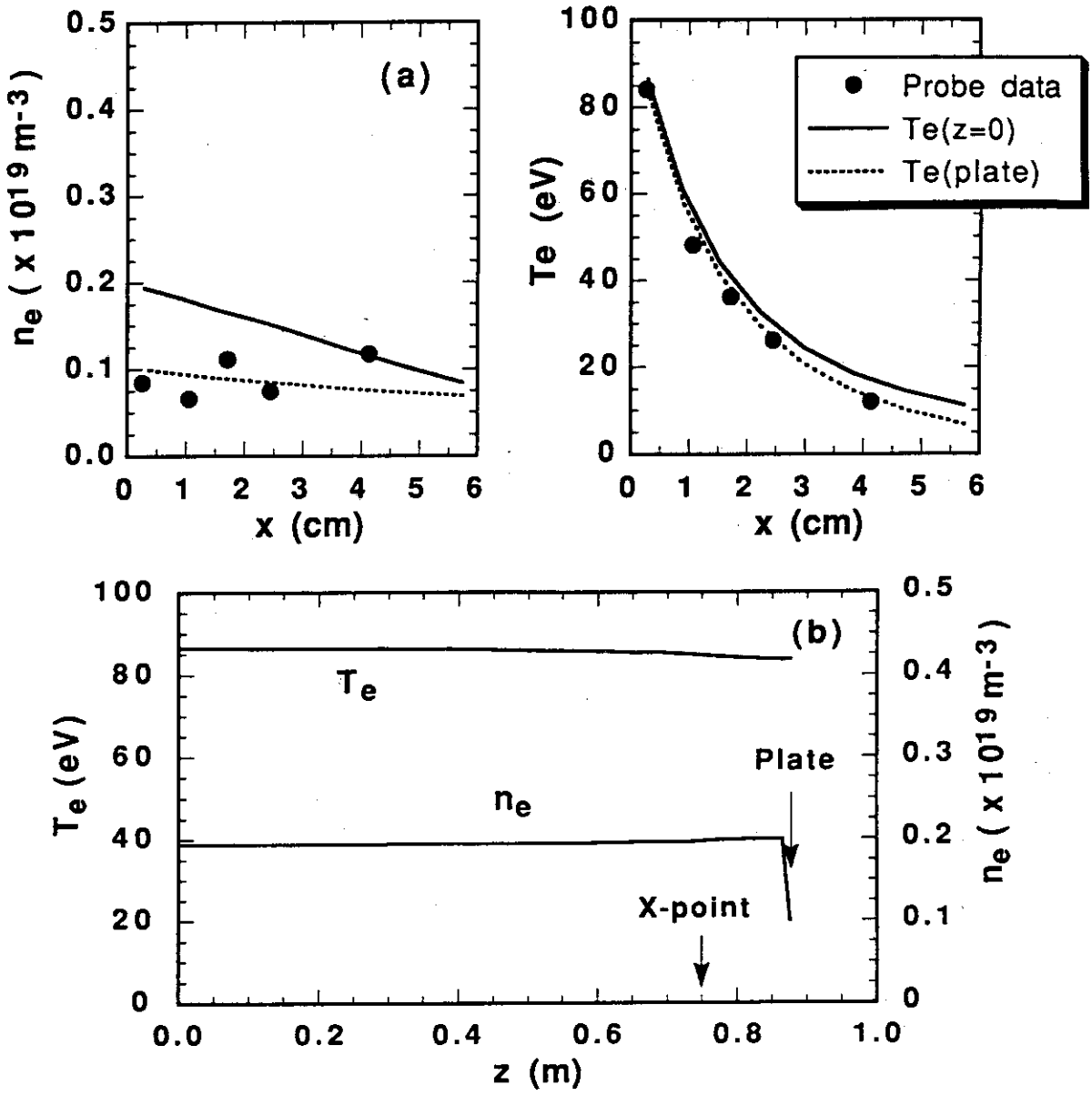

Fig. 6 (a) Radial profiles of temperature and density for the high temperature case. Closed symbols denote the Langmuir probe data. Solid line and broken line represent the calculated profile at the entrance ($\overline{DE}$) and the profile given as the boundary condition at the plate ($\overline{AB}$), respectively.

(b) Calculated profiles of temperature and density in the flux tube close to the separatrix surface for the high temperature case.

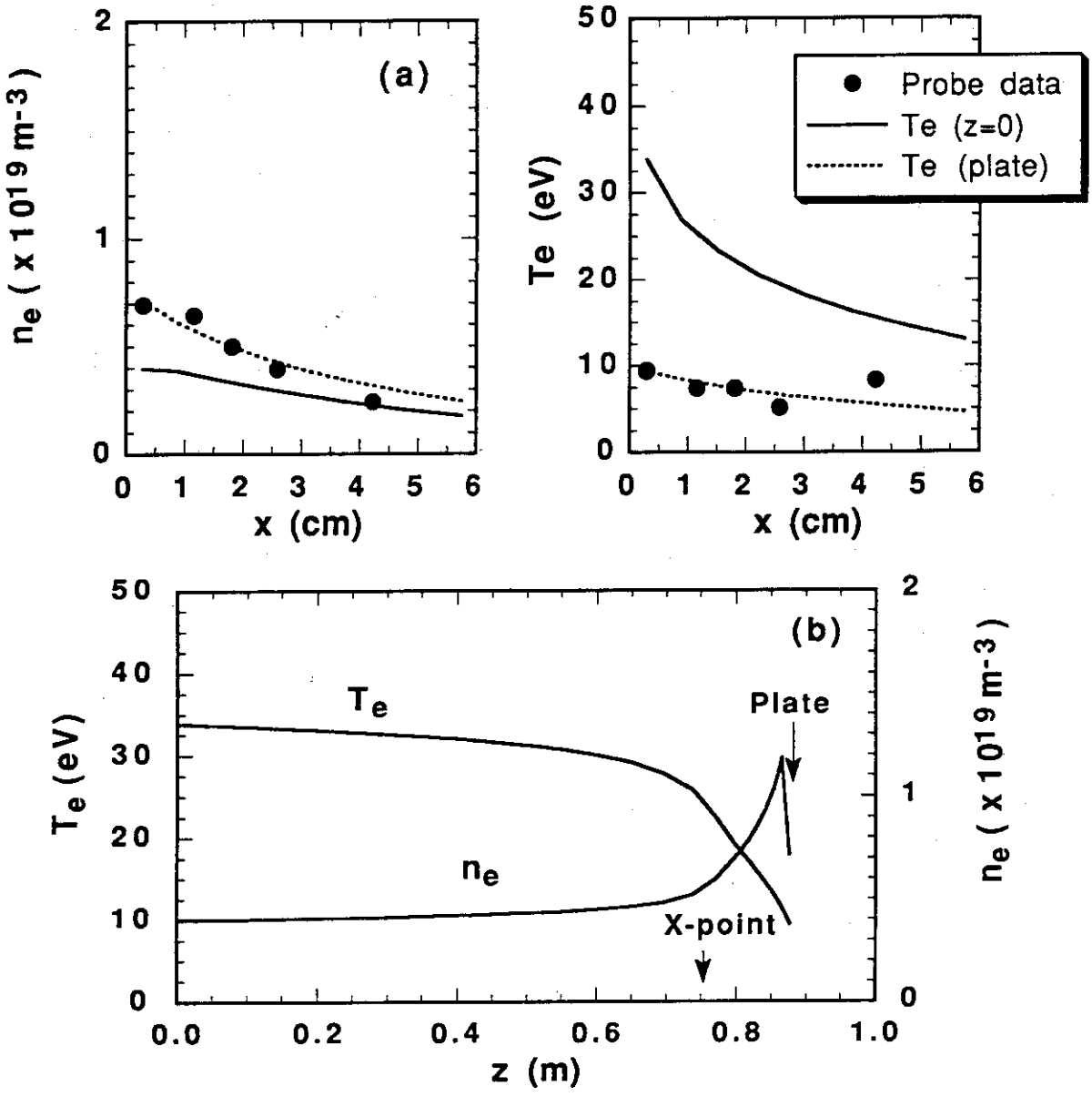

Fig. 7 (a) Radial profiles of temperature and density for the low temperature case. The meanings of symbols and the lines are the same of those in Fig. 6

(b) Calculated profiles of temperature and density in the flux tube close to the separatrix surface for the low temperature case.

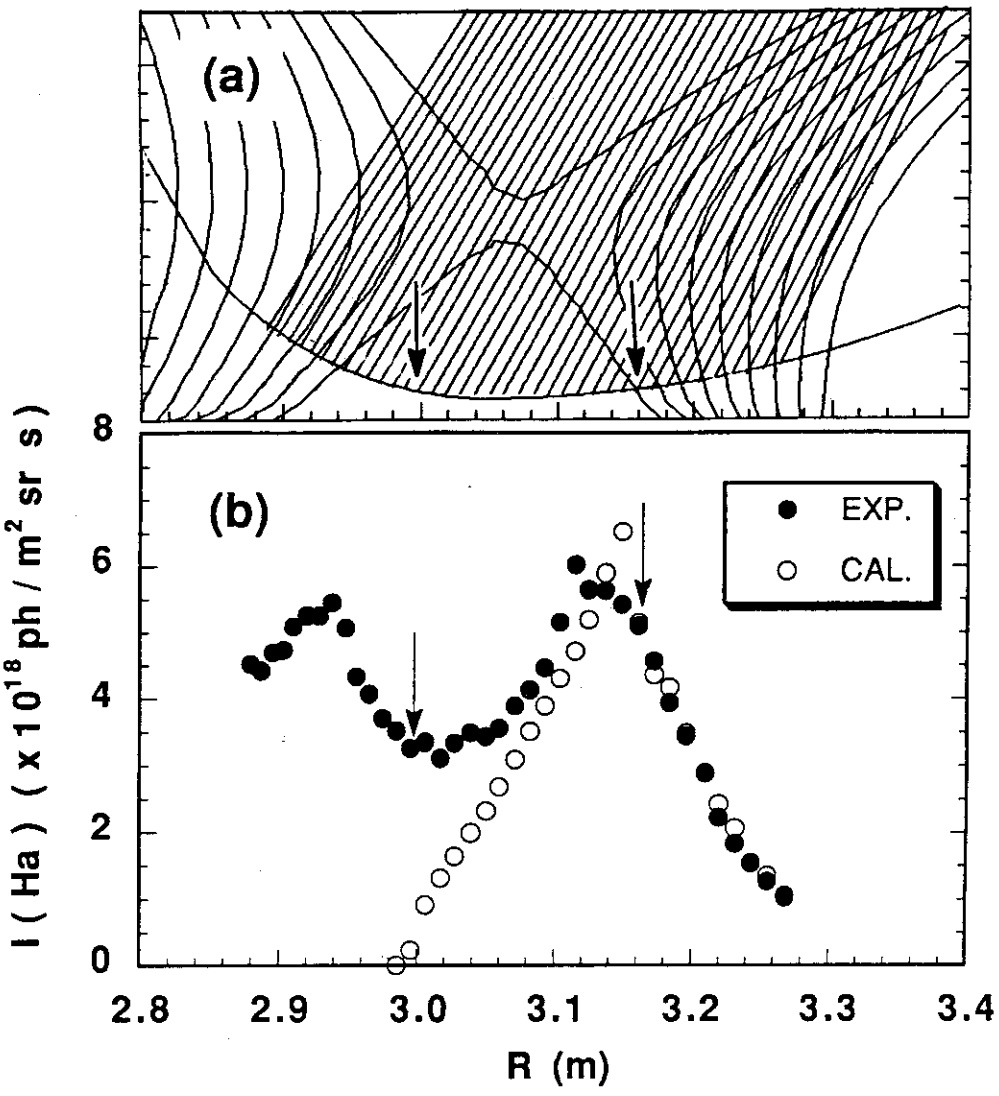

Fig. 8 (a) H_α monitor viewing the divertor plate consists of 38 channels.

(b) Calculated profile of H_α radiation intensity for the low temperature case. The measurement data is also displayed by the closed symbols.